CMOS-coupled NaI scintillation detector for gamma decay measurements

Scott D. Bergeson (ID), Michael J. Ware (ID), and Jeremy Hawk

View Online   Export Citation   CrossMark

CMOS-coupled NaI scintillation detector for gamma decay measurements

Scott D. Bergeson,[1] (iD) Michael J. Ware,[1,a] (iD) and Jeremy Hawk[2]

AFFILIATIONS

[1] BYU Physics and Astronomy, Provo, Utah 84602, USA
[2] Utah Valley Regional Medical Center, Provo, Utah 84602, USA

[a] Author to whom correspondence should be addressed: ware@byu.edu

ABSTRACT

We report an all-solid-state gamma-ray scintillation detector comprised of a NaI(Tl) crystal and a scientific-grade CMOS camera. After calibration, this detector exhibits excellent linearity over more than three decades of activity levels ranging from 10 mCi to 400 nCi. Because the detector is not counting pulses, dead-time correction is not required. Compared to systems that use a photomultiplier tube, this detector has similar sensitivity and noise characteristics on short time scales. On longer time scales, we measure drifts of a few percent over several days, which can be accommodated through regular calibration. Using this detector, we observe that when high activity sources are brought into close proximity to the NaI crystal, several minutes are required for the measured signal to achieve a steady state.

Published under license by AIP Publishing. https://doi.org/10.1063/1.5138208

I. INTRODUCTION

High quality nuclear decay rate measurements require detectors with good sensitivity, stability, and linearity.[1] Depending on the measurement objectives and experimental environment, the detector may also need to provide energy resolution, timing information, and absolute activity levels. Under ideal conditions, activity measurements are limited by Poisson statistics. Generally speaking, higher activity samples or longer measurement times lead to improved precision. However, high activity and long measurement times sometimes compromise the sensitivity, stability, or linearity of the detector.

The stability of the instruments used to measure nuclear decay rates becomes a critical factor when the measurement extends over long time scales.[2,3] For example, it has been suggested that some beta-decay processes might be linked to solar activity.[4] Studies testing this suggestion find that if such variations in decay rates exist, their magnitude is smaller than the precision level of the experiments.[5,6] A long-term experimental measurement using standard detectors in a highly controlled environment found that variation in measured decay rates can also be explained in terms of random variations at the level of detector noise, but that long-term drift of both absolute and relative detection efficiency can limit the certainty of such measurements.[7–9] Improving the stability and

precision of gamma-radiation detectors has the potential to provide results with greater precision in long-term measurements such as those discussed in the references above.

Most gamma-ray measurements can be divided into two processes: The first process converts the gamma radiation into an electronic or photonic signal—ionization in a gas chamber, electron–hole production in a solid, or scintillation in a solid, gas, or liquid. The second process detects and records this electronic or photonic signal, sometimes with additional signal conditioning. These two detection processes sometimes display systematic dependencies on the measurement environment or configuration.[5,7] For example, the measured count rate from a Geiger–Müller tube depends exponentially on the operating voltage. It also depends on the ambient pressure. As another example, scintillation detectors using photomultiplier tubes (PMTs) are unable to reliably measure high activity samples because of excessive dead-time correction. These types of limitations determine the kinds of measurements that these detectors can make.

In this paper, we demonstrate some characteristics of a gamma radiation detector consisting of a NaI(Tl) crystal and a scientific grade camera operating in a mode where the camera is used as a large array of light detectors rather than as a spatial imaging device. We show that this detection system has good stability and acceptable linearity. We also show nonlinearities and instabilities in NaI

scintillation at high activity levels. The regime in which we work uses samples with higher activity than can be used in traditional scintillation measurements due to dead-time issues. This is made possible by the single-photon sensitivity and multi-channel nature of the camera.

II. DETECTOR CHARACTERIZATION

The equipment consists of a scientific camera, a NaI(Tl) scintillator crystal, and a radioactive sample (see Fig. 1). Similar scintillator-camera detector configurations have been used for gamma- and x-ray detection in previous studies.[10–16] However, this work differs from these studies in that the entire camera is used as a "single-channel" detector where the signal from all pixels is summed in a measurement. In this mode of operation, one gives up energy resolution and imaging information in exchange for increased dynamic range, as well as an elimination of dead-time effects since the detection system does not attempt to time-resolve the counts. In principle, the scientific camera could also be used to detect gamma radiation directly, without the scintillation crystal, with the thin silicon camera architecture being used as a kind of proportional detector.[17] However, our detector in this configuration would not be efficient enough for practical use, unlike instruments such as that described in Ref. 18 specifically designed for this mode of operation.

A simplified schematic of our setup is shown in Fig. 1. We use the Andor Neo 5.5 CMOS camera. The camera's CMOS detector is cooled to $-30\,^\circ$C, and the dark signal in the camera is less than 0.1 photo-electrons/pixel/s. The body of the camera (including its processing electronics) is allowed to be at ambient temperature, which
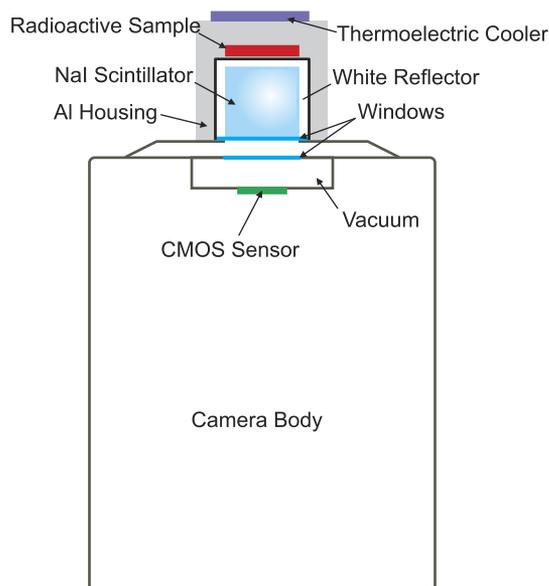
can vary by up to $3\,^\circ$C over our longest datasets, taken over several weeks of time. A cylindrical NaI crystal, 25.4 mm in diameter and 25.4 mm in length (Alpha Spectra model 4 × 4), is attached directly to the lens mount of the camera via a light-tight housing. No focusing optics are used. The crystal is encased in a sealed aluminum housing with a glass window on the end of the cylinder facing the camera, allowing the scintillation photons to be detected with the camera. The distance between the scintillation crystal window and the camera's sensor is 17.5 mm, and the sensor dimensions are 16.6 × 14.0 mm^2. Assuming an 8% loss in reflection at the vacuum window and uniform scintillation throughout the crystal, the geometric ray optics of this arrangement indicate that 8% of the light produced in the crystal will be incident on the sensor. This collection factor could be improved to collect about 10% of the light by placing the crystal directly on the vacuum window, perhaps with some optical grease.

The NaI crystal housing is surrounded with a square aluminum housing with exterior dimensions of 35 × 35 × 50 mm^3, and this aluminum housing is surrounded with thermal insulation to isolate the housing from ambient thermal fluctuations. A thermoelectric cooler (TEC) is mounted on the end of the aluminum housing, as shown in the schematic. A 10 kΩ thermistor is placed in the aluminum housing, and the thermistor and the TEC are connected to a proportional integral differential (PID) controller. The measured in-loop error signal is approximately $\pm 0.002\,^\circ$C. This temperature control stabilizes the light yield from NaI, which varies by about 0.2% per $^\circ$C.[1]

For the long-term stability measurements described below, a radioactive disk source is placed inside the aluminum housing, directly above the scintillator, as shown in the diagram. For the high-activity sample measurements described below, the top portion of the aluminum enclosure was removed, the thermoelectric cooler was moved to the side, and radioactive samples in containers were rested on the top of the scintillator. Gamma radiation from the sample causes scintillation in the crystal, and the scintillation light is detected with the CMOS chip. The measured signal from this detector is the sum of the pixel gray-scale values in each camera image. The data reported here use the camera's high-sensitivity 16-bit digitization mode with an electronic shutter. Our data are measured in units of photoelectrons per pixel per measurement time, which is roughly analogous to average current measurements in an ionization chamber. The well depth per pixels is typically 30 000 electrons according to the manufacturer, so with 16-bit resolution, a change of two in the gray-scale value corresponds approximately to a change of one photoelectron per pixel.

A. Long-term stability

Data from the experiment are shown in Fig. 2(a) over a time period of about 24 days. For these data, we place a 10 μCi Cs-137 D-disk source in direct contact with the NaI crystal housing so that the system approximates a 2π detector. The camera integration time is set to 60 s. For this test, we do not correct for the dark signal, and we do not subtract off the small signal bias associated with the readout process (fixed-pattern read noise). This is a direct test of the uncorrected stability of the scintillator-plus-camera detector. The camera's physical pixels are binned into 8 × 8 "super-pixels," and the average signal per super-pixel, $r(t)$, is close to 5000 in 60 s.

FIG. 1. Schematic of a typical experimental setup. A radioactive sample is placed very near the aluminum housing of a NaI scintillation crystal. The crystal is mounted in a light-tight manner on the top of the camera, directly above the CMOS detector.
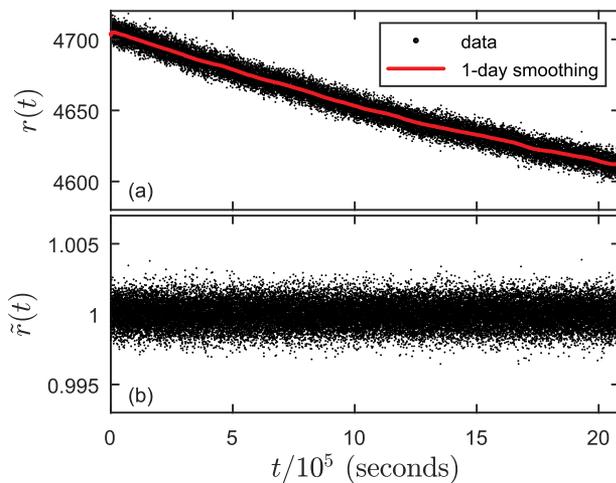
FIG. 2. Data used for stability analysis of the CMOS camera using a 10 μCi Cs-137 gamma source. (a) The measured average signal per pixel per measurement time, $r(t)$, plotted as black dots. Each dot is the average signal over a 60 s interval. We observe a decline of roughly 2%, apparently due to a stability, dark signal, or amplifier gain drift in the camera. Also shown is a line that represents the data smoothed on a one day time scale. (b) The detrended signal, $\tilde{r}(t)$, as defined in the text.

The measured signal in Fig. 2(a) drifts downward by a few percent over the course of the measurement. This downward trend in signal is not due to decay. The half-life of Cs-137 is 30 years, so over the measurement time of Fig. 2, the Cs-137 activity would be expected to change by only 0.01%. Drifts on the scale of a percent over several days were common, and we have observed both positive and negative drifts of similar fractional size while measuring NaI scintillation from long-lived radio-isotopes and also while measuring a strongly attenuated intensity-stabilized laser.

The causes of this long-term drift in are not currently known. The drifts do not appear to correlate simply with ambient temperature, which tends to vary on a daily basis with room use rather than over the long-term trends observed in Fig. 2(a). The drift also did not appear to be improved by attempts at thermal isolation of the detection system. It is not clear if this drift arises from the NaI crystal or from the camera electronics. The precise thermal regulation of the crystal might suggest that the problem lies in the camera.

While the cause of the long-term drift is unknown, it can readily be corrected by regularly calibrating the detector with a known source. This calibration could be automated for a series of long-term measurements. For some situations, ratio measurement techniques could also be used to correct for the drift in long-term measurements, as we have shown in a previous publication.[8] For example, if we consider alternating measurements of two samples over a 4-h time period, a drift of 2% in a week divides out to 0.04% in 4 h.

B. Short-term noise

We can explore the ultimate stability limit of this detection system by separating measurement variability into two different time scales—short-term "noise" and long-term "drift" discussed above.

To remove the long-term drift, we compare the individual data points to the average of the surrounding day's data. This daily smoothing is shown as the solid line in Fig. 2(a). The corrected signal $\tilde{r}(t)$, defined as the ratio of the raw data to the daily smoothing, is plotted in Fig. 2(b).

With the long-term drift removed by dividing by the daily average, we analyze the remaining short-term noise in Fig. 2(b) by averaging the corrected data $\tilde{r}(t)$ over successively longer time intervals and calculating the standard deviation of these averages. The standard deviation of $\tilde{r}(t)$ as a function of the averaging time τ is plotted in Fig. 3. At this signal level, the statistical errors reach below 0.01% in about 2 h of data for the 10 μCi sample. In principle, this level of uncertainty could be reached faster by measuring a sample with higher activity.

We compared the short-term noise characteristics observed in Figs. 2(b) and 3 to a separate set of data collected by the PMT-based detection system described in Ref. 7. This comparison dataset was measured using a PMT-based system comprised of a standard NaI scintillating crystal (Saint-Gobain 2M2/2-X) coupled with a standard PMT detector (Ortec Digibase PMT/MCA) for a separate experiment.[7] In that work, a 10 μCi Eu-154 source (half-life of 8.6 years) was placed about 1 cm above the detector, and the entire detection system was placed inside a temperature, humidity, and pressure controlled chamber as part of a long-term decay measurement. The total signal $r(t)$ in each 300 s interval is plotted in Fig. 4(a), along with a fit of the data to a single exponential decay. Figure 4(b) plots $\tilde{r}(t)$ for this comparison dataset, where $\tilde{r}(t)$ is now defined as the ratio of the signal to the exponential fit, for comparison to Fig. 3(b). While the sensitivity of the detection system for this comparison dataset will be different, our purpose here is to compare system stability rather than sensitivity.

The 300 s integration time for the Eu-154 comparison dataset is different from the 60 s integration time in Fig. 3, which is the reason for the decreased noise level in Fig. 4. When the data in Fig. 3 are binned in 300 s time intervals (by summing five adjacent 60 s intervals), the noise level for the new CMOS data is only slightly lower than that for the PMT-based data: a standard deviation of 0.04% for the CMOS $\tilde{r}$ data vs a standard deviation of 0.05% for the PMT $\tilde{r}$ data. The low level of short-term noise in the new CMOS-based systems indicates that if the long-term drift issues can be
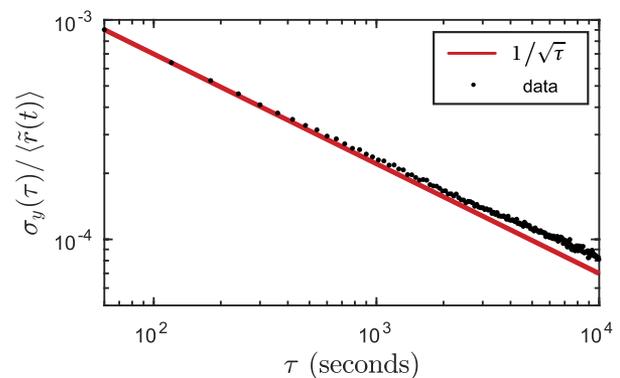

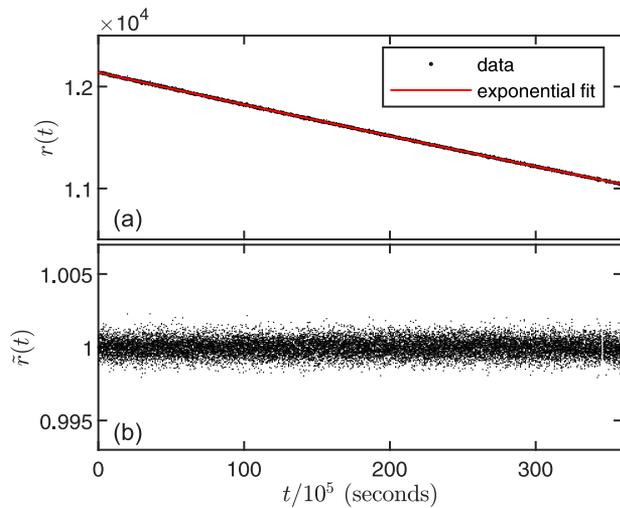**FIG. 3**. The standard deviation of the detrended data in Fig. 2(b) as a function of the averaging time τ.

FIG. 4. Comparison data used from a NaI scintillation system monitoring a 10 μCi Eu-154 gamma source. (a) The average signal per pixel per 300 s measurement time, $r(t)$, plotted as black dots. The decline in signal is due to natural decay, and the line is a fit to a single exponential decay. (b) The detrended signal, $\tilde{r}(t)$, given by the data divided by the exponential fit. The smaller noise in this detrended signal when compared to Fig. 2 is due entirely to the longer integration time per data point.

corrected, this new detection system has the potential to have very low noise.

C. System linearity

We characterize the linearity of the detection system by measuring the decay of short-lived radio-isotopes over several half-lives. Measurements of Tc-99m, with a half-life of $\tau_{1/2} = 6.0067 \pm 0.0010$ h, and F-18, with a half-life of $\tau_{1/2} = 1.828\,90 \pm 0.000\,23$ h,[19] are shown in Fig. 5. These samples contain the radio-isotopes in a liquid form as a pertechnetate for Tc-99m or fludeoxyglucose for F-18. These samples are held in a sealed plastic syringe above the NaI crystal. The crystal subtends a solid angle of 1.0 sr. In this configuration, a 10 mCi sample exposes the crystal to 3×10^7 gammas per second.

In Fig. 5(a), we show the measured decay signal (black dots) and the expected decay signal (red line) for a 3 mCi Tc-99m source. The scintillation data are recorded using the camera's 16-bit image mode. In this mode, the camera uses a dual-amplifier configuration to achieve the maximum dynamic range: One amplifier is optimized for large signals and the other is optimized for low signals. These amplifiers are not perfectly matched, causing a slight decrease in system response for signal levels below an intermediate value. This explains why the measured signal level in Fig. 5(a) falls below the known exponential decay.

We use the measured 3 mCi Tc-99m signal plotted in Fig. 5(a) to linearize the overall system response. The ratio of the measured signal to the known exponential decay gives a signal-dependent correction function that is applied to subsequent measurements. In Fig. 5(b), we apply this correction to four measurements of Tc-99m samples with different activities (10 mCi, 0.4 mCi, 0.07 mCi, and
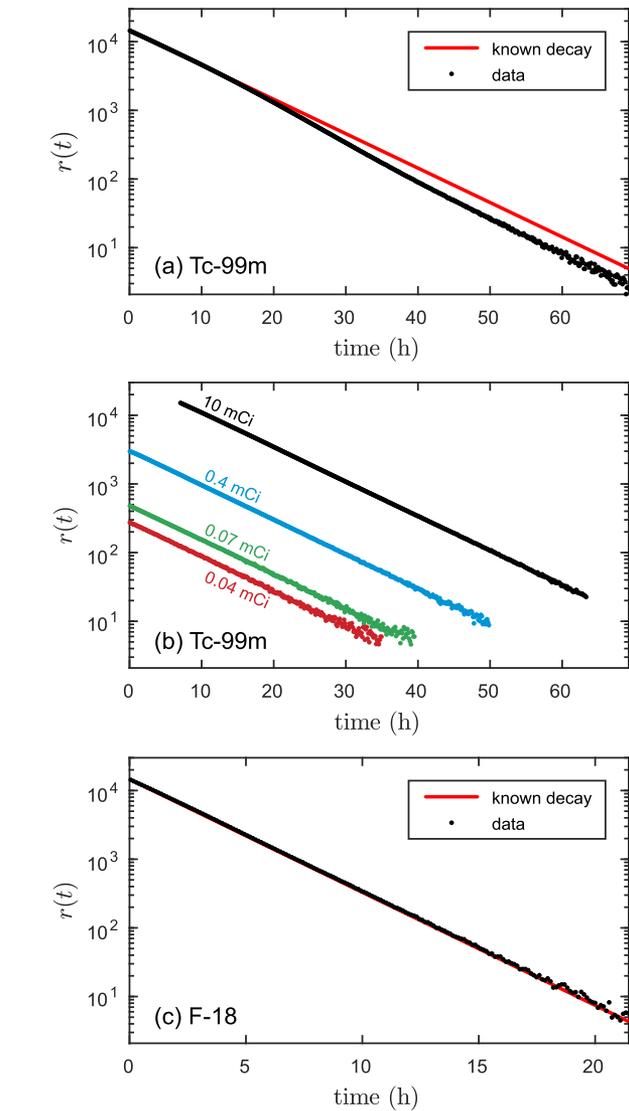

FIG. 5. Linearity measurements and correction using short-lived radio-isotopes. (a) Tc-99m. The black dots are the measured signal, and the red line shows the expected signal using the known half-life. The departure from exponential decay is due to amplifier nonlinearity in the camera. The initial sample activity is approximately 3 mCi. (b) Tc-99m data with the linearization correction applied. The four fitted half-lives from these samples average to 6.00(2) days, close to the accepted value of 6.0067(10) days. (c) F-18 data. The raw data are linearized using the Tc-99m correction. This produces a F-18 half-life that is within 1% of the accepted value. The black dots are the linearized data, and the red line is a fit with the known decay half-life. The initial F-18 sample activity is about 3 mCi.

0.04 mCi). The linearization reproduces the known half-life with sub-percent residuals.

The linearization function is signal dependent, independent of the isotope. In Fig. 5(c), we show the measured signal from a 3 mCi F-18 source with the same correction function applied. The fitted lifetime matches the known lifetime with an error of less than 1%.

As an additional check of the system linearity, we measure the signal from several I-125 seeds. This isotope is a low-energy gamma emitter with a half-life of 59.388(28) days.[19] We place different activity samples in front of the NaI crystal and measure the system response. The ratio of the measured response to the known source activity matches the linearity function obtained from the Tc-99m measurements to within the experimental uncertainties.

Note that this detection system is immune to pulse pile-up and dead time systematics. This is demonstrated in Fig. 5, where samples ranging from 0.04 mCi to 10 mCi can be measured without using any dead time correction. These measurements correspond to signal levels that are far higher than can be measured with traditional PMT-based counting detectors and after the linearization procedure described above show excellent linearity over four decades of dynamic range.

III. TIME RESPONSE OF SODIUM IODIDE

Finally, we turn to the time-dependence of the NaI scintillation crystal when measuring high activity samples. Data in Fig. 6 show the measurement data $r(t)$ of the first two hours of three different Tc-99m samples, normalized by the initial signal $r(0)$ measured just after the sample is placed on the detector. These data are taken from the same datasets used in Fig. 5. However, for that plot, the first few hours of nonlinear behavior were not used.

Figure 6 shows a nonlinear response of the NaI scintillation, which increases with an increase in activity levels. Rather than immediately showing the decay of the source in signal, the crystal's response initially increases in time until the expected decay behavior is observed. For samples with higher activity rates, more time is required for this effect to subside. For the samples used in this study, this can take as long as a few hours. The time scale of this effect is much longer than the typical relaxation times
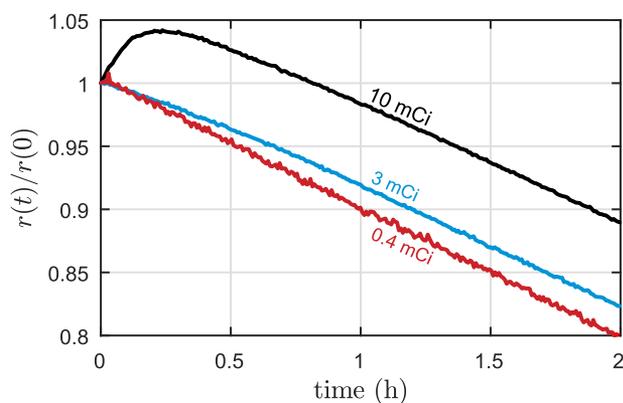
observed for NaI(Tl). The light pulse shape for NaI(Tl) has a typical decay time on the scale of hundreds of nanoseconds.[1] While some relaxation times have been observed on the millisecond time scale,[20] these are also much too short of a time scale to explain this effect.

This initial nonlinear response of the detection system makes it inconvenient to use a NaI-based scintillation detector to measure high-activity samples. We have not found this effect documented in the literature, perhaps due to the high activity rates needed to observe it. It may also be the result of some undiagnosed systematic effect in our measurement system. The techniques used to correct for the long-term stability issues discussed in Sec. II A (regular calibration or ratio techniques) work best when the detector can quickly measure high-precision statistics for high activity samples on a short (less than an hour) time scale. Unfortunately, this is precisely the time scale for short-term drifts in the NaI response shown in Fig. 6. However, when steady state is reached, the analysis in Fig. 5 suggests that the decay of the short-lived Tc-99m and F-18 isotopes can be accurately measured.

IV. CONCLUSION

We have measured the characteristics of a gamma-radiation detector based on a NaI crystal and a scientific camera used as an array of parallel detectors. The system is capable of measuring high activity levels without dead time correction. With proper linearization, this detector accurately measures short-lived radioisotopes over three decades of dynamic range. We observe short-term changes in the NaI scintillation level at high activity. We also observe long-term instabilities of a few percent that may be attributable to the camera, the NaI crystal, or both. These drift characteristics must be considered for high precision measurements of the nuclear decay rates.

Future work will be needed to isolate the source of long-term drift seen in Fig. 2. The camera could be tested in a temperature-controlled environment using an intensity-controlled light source of verified stability. Future work should also study the response linearity of other suitable scintillation materials. The analysis in Fig. 3 suggests that it should be possible to reach a fractional accuracy of 0.0003% in 7 days for a 1 mCi sample, assuming that all sources of drift have been corrected. The camera-based detection system is capable of measuring even higher activity sources. However, it will require a more linear scintillator than NaI.

FIG. 6. Measurements of three different Tc-99m samples for the first two hours. The three measurements have been normalized so that the data overlap at time zero, when the sample is first placed on the detector. The 0.4 mCi source closely approximates the expected Tc-99m decay. The time-dependent intensity nonlinearity increases with sample activity, and more time is required before the data approach the expected exponential decay. Using laboratory light sources, we verify that this behavior is not due to the camera but rather arises from the NaI crystal itself. Note that the early time data leading to this effect were not included in the linearity measurements of Fig. 5.

REFERENCES

[1] G. F. Knoll, *Radiation Detection and Measurement*, 4th ed. (Wiley, 2010).

[2] J. H. Jenkins, E. Fischbach, J. B. Buncher, J. T. Gruenwald, D. E. Krause, and J. J. Mattes, "Evidence of correlations between nuclear decay rates and Earth–Sun distance," Astropart. Phys. **32**(1), 42–46 (2009).

[3] O. Nähle and K. Kossert, "Comment on "Comparative study of beta-decay data for eight nuclides measured at the Physikalisch-Technische Bundesanstalt" [Astropart. Phys. 59 (2014) 47–58]," Astropart. Phys. **66**, 8–10 (2015).

[4] P. Sturrock, G. Steinitz, E. Fischbach, A. Parkhomov, and J. Scargle, "Analysis of beta-decay data acquired at the Physikalisch-Technische Bundesanstalt: Evidence of a solar influence," Astropart. Phys. **84**, 8–14 (2016).

[5] S. Pommé, H. Stroh, J. Paepen, R. V. Ammel, M. Marouli, T. Altzitzoglou, M. Hult, K. Kossert, O. Nähle, H. Schrader, F. Juget, C. Bailat, Y. Nedjadi, F. Bochud, T. Buchillier, C. Michotte, S. Courte, M. van Rooy, M. van Staden, J. Lubbe, B. Simpson, A. Fazio, P. D. Felice, T. Jackson, W. V. Wyngaardt,

M. Reinhard, J. Golya, S. Bourke, T. Roy, R. Galea, J. Keightley, K. Ferreira, S. Collins, A. Ceccatelli, M. Unterweger, R. Fitzgerald, D. Bergeron, L. Pibida, L. Verheyen, M. Bruggeman, B. Vodenik, M. Korun, V. Chisté, and M.-N. Amiot, "Evidence against solar influence on nuclear decay constants," Phys. Lett. B **761**, 281–286 (2016).

[6] H. Schrader, "Seasonal variations of decay rate measurement data and their interpretation," Appl. Radiat. Isot. **114**, 202–213 (2016).

[7] M. J. Ware, S. D. Bergeson, J. E. Ellsworth, M. Groesbeck, J. E. Hansen, D. Pace, and J. Peatross, "Instrument for precision long-term β-decay rate measurements," Rev. Sci. Instrum. **86**(7), 073505 (2015).

[8] S. Bergeson, J. Peatross, and M. Ware, "Precision long-term measurements of beta-decay-rate ratios in a controlled environment," Phys. Lett. B **767**, 171–176 (2017).

[9] Q. McKnight, S. Bergeson, J. Peatross, and M. Ware, "2.7 years of beta-decay-rate ratio measurements in a controlled environment," Appl. Radiat. Isot. **142**, 113–119 (2018).

[10] S. Caccia, G. Bertuccio, D. Maiocchi, P. Malcovati, N. Ratti, and D. Martin, "A mixed-signal spectroscopic-grade and high-functionality cmos readout cell for semiconductor x-γ ray pixel detectors," IEEE Trans. Nucl. Sci. **55**(5), 2721–2726 (2008).

[11] D. Meier, A. Czermak, P. Jalocha, B. Sowicki, M. Kowal, W. Dulinski, G. Maehblum, E. Nygard, K. Yoshioka, J. Fuster, C. Lacasta, M. Mikuz, S. Roe, P. Weilhammer, C. H. Hua, S. J. Park, S. J. Wildermann, L. Zhang, N. H. Clinthorne, and W. L. Rogers, "Silicon detector for a Compton camera in nuclear medical imaging," in *2000 IEEE Nuclear Science Symposium. Conference Record (Cat. No.00CH37149)* (IEEE, 2000), Vol. 3, pp. 22/6–2210.

[12] B. W. Miller, S. J. Gregory, E. S. Fuller, H. H. Barrett, H. B. Barber, and L. R. Furenlid, "The iQID camera: An ionizing-radiation quantum imaging detector," Nucl. Instrum. Methods Phys. Res., Sect. A **767**, 146–152 (2014).

[13] C. Stapels, W. G. Lawrence, J. Christian, M. R. Squillante, G. Entine, F. L. Augustine, P. Dokhale, and M. McClish, "Solid-state photomultiplier in CMOS technology for gamma-ray detection and imaging applications," in *IEEE Nuclear Science Symposium Conference Record, 2005* (IEEE, 2005), Vol. 5, pp. 2775–2779.

[14] B. W. Miller, L. R. Furenlid, S. K. Moore, H. B. Barber, V. V. Nagarkar, and H. H. Barrett, "System integration of fastSPCET III, a dedicated SPCET rodent-brain imager based on Bazookaspect detector technology," in *2009 IEEE Nuclear Science Symposium Conference Record (NSS/MIC)* (IEEE, 2009), pp. 4004–4008.

[15] C. M. Michail, V. A. Spyropoulou, G. P. Fountos, N. I. Kalyvas, I. G. Valais, I. S. Kandarakis, and G. S. Panayiotakis, "Experimental and theoretical evaluation of a high resolution CMOS based detector under x-ray imaging conditions," IEEE Trans. Nucl. Sci. **58**(1), 314–322 (2011).

[16] M. Nikl, "Scintillation detectors for x-rays," Meas. Sci. Technol. **17**, R37 (2006).

[17] T. E. Peterson and L. R. Furenlid, "SPECT detectors: The anger camera and beyond," Phys. Med. Biol. **56**, R145 (2011).

[18] F. Lebrun, J. P. Leray, P. Lavocat, J. Crétolle, M. Arquès, C. Blondel, C. Bonnin, A. Bouère, C. Cara, T. Chaleil, F. Daly, F. Desages, H. Dzitko, B. Horeau, P. Laurent, O. Limousin, F. Mathy, V. Mauguen, F. Meignier, F. Molinié, E. Poindron, M. Rouger, A. Sauvageon, and T. Tourrette, "ISGRI: The INTEGRAL soft gamma-ray imager," Astron. Astrophys. **411**, L141–L148 (2003); arXiv:astro-ph/0310362.

[19] See http://www.nucleide.org/DDEP_WG/DDEPdata.htm for Laboratoire Henri Bacquerel, Recommended Values; accessed 23 September 2016.

[20] M. Itoh, S. Hashimoto, and N. Ohno, "Self-trapped exciton luminescence in dilated nai crystals–relaxation process of excitons in alkali halides–," J. Phys. Soc. Jpn. **60**(12), 4357–4365 (1991).